Effects of front surface plasma expansion on proton acceleration driven by the Vulcan Petawatt laser

D. C. Carroll, M. N. Quinn, X. H. Yuan and P. McKenna

SUPA, Department of Physics, University of Strathclyde, Glasgow G4 0NG, UK

O. Lundh and C.-G. Wahlström

Department of Physics, Lund University, P.O. Box 118, S-22100 Lund, Sweden

F. Nürnberg and M. Roth

Institute for Nuclear Physics, Darmstadt University of Technology, Darmstadt, Germany

Contact | **p.mckenna@phys.strath.ac.uk**

K. Markey, S. Kar and M. Zepf

School of Mathematics and Physics, Queen's University Belfast, Belfast BT7 1NN, UK

S. Bandyopadhyay, D. Pepler and D. Neely

Central Laser Facility, STFC, Rutherford Appleton Laboratory, HSIC, Didcot, Oxon OX11 0QX, UK

R. G. Evans

The Blackett Laboratory, Imperial College London, London SW7 2AZ, UK

R. Jafer, R. Redaelli and D. Batani

Dipartimento di Fisica, Università di Milano Bicocca, 20126 Milano, Italy

Introduction

Multi-MeV ion acceleration driven by high power laser irradiation of thin foil targets continues to attract considerable international interest [1]. At the laser intensities presently available, ions are accelerated by the Target Normal Sheath Acceleration mechanism [2]. The proton, due to its high charge-to-mass ratio, is the most efficiently accelerated ion species, and is sourced from hydrogenated layers on the target surfaces. A number of potential applications, including proton oncology, radiography, lithography and proton based fast ignition have been suggested for this novel and potentially compact laser-driven source. The challenge now is to develop techniques to enhance and control the source and beam properties. In particular, the development of techniques based on optical control of the acceleration would enable applications requiring the delivery of proton pulses at high repletion rate.

The properties of the proton beam are sensitive not only to the high power laser pulse, but also any prepulses or Amplified Spontaneous Emission (ASE) at its leading edge. This typically preheats the front surface of the target creating plasma expansion. In the case of sufficiently thin targets, the rear surface of the target may also be preheated, which reduces the maximum energy of the accelerated protons [3, 4]. In addition, Lindau *et al.* [5] have shown that the direction of the beam of accelerated protons is also sensitive to the ASE level and timing. Even if the target is sufficiently thick that the rear surface is unperturbed, plasma expansion at the front surface can significantly affect rear surface ion acceleration. It has been shown in recent Particle-In-cell (PIC) simulation studies that laser absorption efficiency, and therefore proton acceleration, can be enhanced by controlling the scale length of the front surface preplasma [6-9]. This has also been observed experimentally for proton acceleration driven by ultrashort (tens of femtosecond) laser pulses focused to intensities between 10^{18} and 10^{19} W/cm^2 [10, 11].

Here we report on an experimental investigation of the effects of front surface plasma expansion on proton acceleration driven by ultraintense (3×10^{20} W/cm^2) picosecond laser pulses, for which the highest energy protons are presently produced [12]. This laser pulse regime, intensity and pulse duration, is also directly relevant to the fast ignition approach to fusion energy [13].

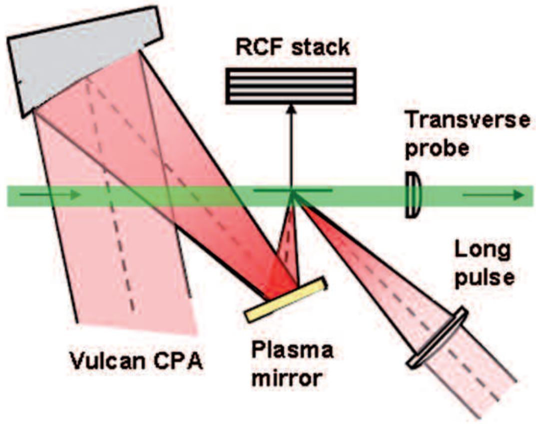

Figure 1. Experiment arrangement. Proton acceleration is driven by the Vulcan petawatt CPA laser, with contrast enhancement provided using a plasma mirror positioned in the focusing beam. Plasma expansion at the target front surface is produced by one of the main six Vulcan long pulse (nanosecond) beams and characterised using a frequency doubled transverse optical probe.

Experimental

The experiment was carried out in Vulcan Target Area Petawatt using the Chirped Pulse Amplified (CPA) short pulse beam and the recently installed long pulse beam. Figure 1 shows a schematic of the arrangement. The CPA, 1054 nm wavelength (λ), pulses were used to drive the acceleration of protons. The intensity of the ASE pedestal was suppressed to ~10^{11} W/cm^2 using a plasma mirror [14], positioned in the focusing beam. The mirror reflected 32% of the beam energy onto the target. The maximum energy on target was 115 J, focused to a spot size of 5 μm (FWHM), giving a calculated peak intensity, I_{CPA}, equal to 3×10^{20} W/cm^2.

Plasma formation at the target front surface was induced using laser pulses of 6 ns duration (rise time equal to 0.2 ns) and wavelength equal to 1054 nm. An f/10 lens was used to focus the beam to an approximately flat-top intensity distribution with a diameter, at the target surface, equal to 450 μm, centered on the position of the CPA focus. The energy of the 'ablation pulse' was varied to produce intensity, I_{abl}, in the range 0.5 to 5 TW/cm^2. The delay of the CPA pulse, Δt, with respect to the arrival of the ablation pulse on target was varied in the range 0.5 to 3.6 ns, with 0.2 ns precision.

The targets were either 25 μm-thick planar Cu foils or 25 μm-thick planar Au foils with a periodic groove structure (lines) on the rear surface (see separate report by F. Nürnberg *et al.*[21] for details of the structured targets). Stacked dosimetry film, positioned at the rear of the target, was used to measure the spatial and energy distributions of the beam of accelerated protons.

Characterisation of plasma expansion

The plasma expansion at the target front surface was measured using transverse optical probe interferometry. A small fraction of the main CPA beam is diverted, frequency doubled and directed along the surface of the target. A Nomarski interferometer, involving a Wollaston prism and polarizer was used[15]. Interferograms of the plasma expansion were recorded with a spatial resolution of 5 μm, 5 ps after the arrival of the CPA pulse. Phase shifts, due to the change in refractive index in the region of plasma expansion, were retrieved by application of a 2-D Fast Fourier Transform. The transverse electron density profile was retrieved by calculation of Abel Inversion, assuming cylindrical symmetry.

Figure 2 shows the retrieved on-axis electron densities of the expanding plasma for I_{abl} in the range 0.5 to 5 TW/cm^2, for fixed Δt=0.5 ns. As expected, the plasma expands faster when heated at higher intensities, creating a longer plasma scale length. The upper limit on the measured density profile, ~4×10^{19} cm^{-3}, is due to refraction in the steep density gradients. We refer to the measured scale length of the electron density in the underdense *outer* part of the expanding plasma as L_O and the scale length in the *inner* region, near the critical density, as L_I. L_O is retrieved by fitting the equation $n_e(x)=n_0\times\exp(-x/L_O)$ (where n_e is the electron density and x is the distance from the target surface) to the measured electron density profile, and is found to scale with $I_{abl}^{0.6}$.

Two-dimensional hydrodynamic simulations were performed, using the Pollux code[16], to calculate the full initial density profile of the target. Cylindrical symmetry was used with a 300 μm × 300 μm grid. The laser wavelength and spot radius were set at 1.06 μm and 220 μm, respectively, and a laser pulse with a rise time of 0.2 ns was used, to match the experimental parameters.

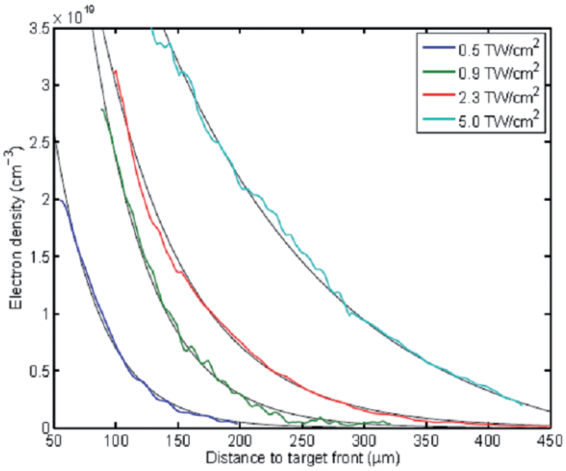

Figure 2. Measured electron density profile on-axis for given ablation pulse intensities.

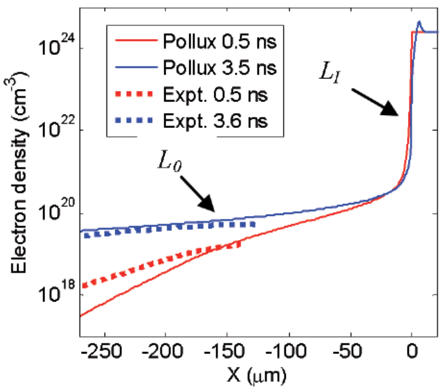

Figure 3. Solid lines are the calculated (using the Pollux hydrodynamic code) electron density profiles at the front surface of a Cu target for different expansion times (0.5 ns and ~3.5 ns) at fixed I_{abl}=1 TW/cm^2. Dashed lines are the corresponding experimental measurements obtained from the transverse optical probe. X=0 corresponds to the initial target front surface.

Good agreement is observed between the calculated and measured density profiles, as shown in the example results in figure 3. Two distinct regions of preplasma expansion, with scale lengths L_I and L_O, are clearly observed. Over the range of ablation pulse parameters investigated experimentally, L_O is found to increase up to 200±40 μm. By contrast, L_I increases only up to ~1 μm, representing only a small change in the overall thickness of the overdense region of the target.

Importantly, the upper limits of I_{abl} and Δt were chosen such that the shock wave launched into the target by the ablation pressure does not reach the rear surface to influence the ion acceleration. This is confirmed in the hydrodynamic simulation results. Experimentally, it is also confirmed by the transverse optical probe measurements, and by the mapping of the structure machined on the rear surface into the measured spatial intensity distribution of the proton beam.

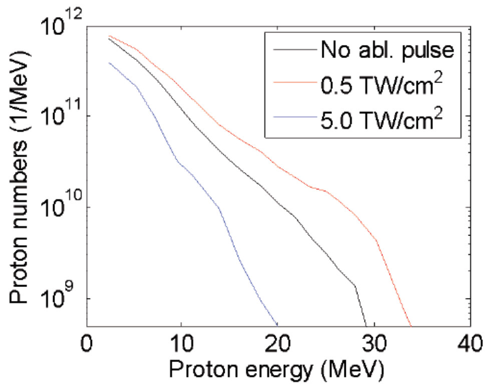

Figure 4. Example proton energy spectra for different I_{abl} and fixed Δt=0.5 ns.

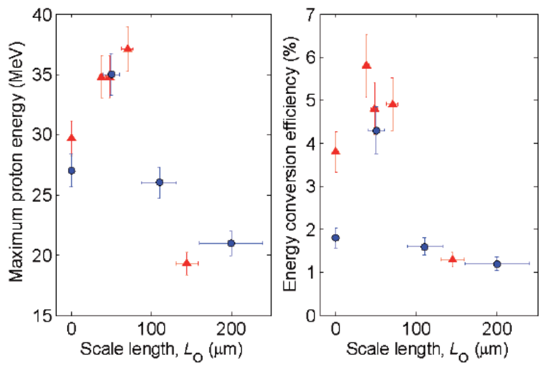

Figure 5. Maximum proton energy and laser-to-proton energy conversion efficiency as a function of L_O, obtained for different I_{abl} up to 5.0 TW/cm^2 for fixed Δt=0.5 ns (red), and for different Δt up to 3.6 ns for fixed I_{abl} (blue).

Effects on proton acceleration

The spectral and spatial intensity distributions of the beam of accelerated protons are measured as a function of (1) I_{abl} for fixed Δt=0.5 ns, and (2) Δt for fixed I_{abl}=1 TW/cm^2. The CPA pulse and target parameters are fixed for both scans. Figure 4 shows example proton energy spectra from a scan of I_{abl}. Typically, compared to the case of steep density gradient, we observe significant increases in the proton flux, temperature and maximum energy for conditions corresponding to L_O ~30 to 60 μm. For L_O >100 μm, a decrease in all three beam parameters, below their respective values for the case of a sharp density gradient, is observed. As shown in figure 5, the same dependency is observed whether L_O is changed by variation of I_{abl} or Δt. These observations clearly indicate that there exists an optimum preplasma expansion for enhancing the proton flux and energy.

The example transverse optical probe measurements of figure 6 clearly show that the propagation of the CPA pulse in the outer region of the expanding plasma changes significantly with increasing plasma scale length. For some shots, for the conditions in which the peak in the maximum proton energy and conversion efficiency are produced, the CPA pulse propagation is observed as a single channel, with width smaller than the nominal focusing cone of the CPA beam. This is evidence of self-focusing, which would lead to an increase in the laser intensity near the critical density surface. By contrast, for very long scale length expansion (L_O>100 μm) the propagating CPA pulse is observed to break up, resulting in multiple filaments, with energy deposited over a larger area that the nominal CPA laser focal spot, thus reducing the laser intensity. These observations qualitatively agree with the observed changes to the proton maximum energy, which scales with $(I_{CPA}\lambda^2)^{0.5}$ [17].

By contrast, we observe that the proton beam circularity and uniformity continue to increase with increasing scale length. The improvements in these beam parameters are consistent with our previous observations reported in Carroll *et al.* [18], and further work is required to understand what gives rise to these improvements in beam quality.

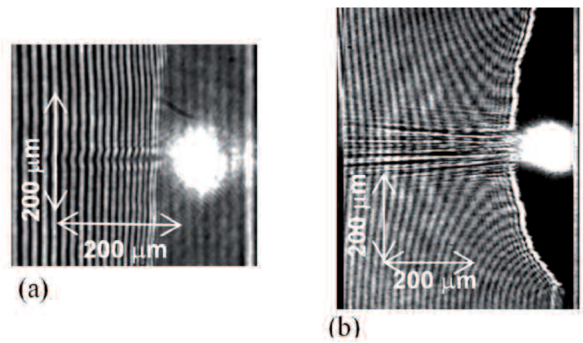

Figure 6.(a) Example interferometric probe image showing channeling of the CPA laser beam in relatively short scale length preplasma; (b) Example interferometric probe image showing break-up of the CPA laser beam in long scale length preplasma. The laser pulses are incident from the left.

Conclusions

In summary, we have directly measured the effects of preplasma expansion on proton acceleration for the ultraintense, picosecond laser pulse regime. Compared to a sharp density gradient, a preplasma with an underdense scale length of ~30 to 60 μm enhances proton acceleration due to increased energy absorption and self-focusing of the laser. The observed enhancement in the maximum energy is in good agreement with that predicted by Sentoku *et al.* [6] for the pulse intensity and wavelength used in the experiment. As the preplasma scale length increases to ~150 μm break-up of the propagating laser pulse reduces the laser intensity near the critical surface and giving rise to increased proton beam uniformity, but with reduced energy and flux.

Acknowledgements

We acknowledge the expert support of the staff at the Central Laser Facility. This work was supported by EPSRC and the EU COST P-14 Action.

References

1. M. Borghesi *et al.*, *Fusion Science and Technology* **49**, 412 (2006).
2. S. C. Wilks *et al.*, *Physics of Plasmas* **8**, 542 (2001).
3. M. Roth *et al.*, *Physical Review Special Topics-Accelerators and Beams* **5**, 061301 (2002).
4. J. Fuchs *et al.*, *Physical Review Letters* **99**, 015002 (2007).
5. F. Lindau *et al.*, *Physical Review Letters* **95**, 175002 (2005).
6. Y. Sentoku *et al.*, *Applied Physics B* **74**, 207 (2002).
7. J. T. Seo, S. H. Yoo, and S. J. Hahn, *Journal of the Physical Society of Japan* **76**, 114501 (2007).
8. H. J. Lee *et al.*, *Physics of Plasmas* **11**, 1726 (2004).
9. A. A. Andreev *et al.*, *Plasma Physics and Controlled Fusion* **48**, 1605 (2006).
10. A. Maksimchuk *et al.*, *Physical Review Letters* **84**, 4108 (2000).
11. A. Yogo *et al.*, *Physics of Plasmas* **14**, 0431104 (2007).
12. L. Robson *et al.*, *Nature Physics* **3**, 58 (2007).
13. M. Tabak *et al.*, *Physics of Plasmas* **1**, 1626 (1994).
14. B. Dromey *et al.*, *Review of Scientific Instruments* **75**, 645 (2004).
15. R. Benatter, C. Popovics, and R. Sigel, *Review of Scientific Instruments* **50**, 1583 (1979).
16. G. J. Pert, *Journal of Computational Physics* **43**, 111 (1981).
17. S. C. Wilks *et al.*, *Physical Review Letters* **69**, 1383 (1992).
18. D. Carroll *et al.*, *Physical Review E* **76**, 065401 (2007).
19. R. Hemker, *PhD thesis* UCLA (2000).
20. P. Gibbon *et al.*, *Physics of Plasmas* **6**, 947 (1999).
21. F. Nürnberg *et al.*, CLF Annual Report 2007/2008.